

SENSITIVITY REACH ON ANOMALOUS HIGGS COUPLINGS VIA TRIPHOTON PRODUCTION FOR THE POST-LHC CIRCULAR HIGH-ENERGY HADRON COLLIDERS*

H. DENIZLI[†], A. SENOL[‡]

Department of Physics, Bolu Abant Izzet Baysal University, 14280 Bolu, Turkey

(Received April 1, 2021; accepted November 3, 2021)

The potential of triphoton production to obtain limits on anomalous Higgs boson couplings at $H\gamma\gamma$ and $HZ\gamma$ vertices is studied in the Standard Model Effective Field Theory (EFT) framework for the post-LHC circular high-energy hadron colliders: High Luminosity-LHC (HL-LHC), High-Energy LHC (HE-LHC), and Low-Energy FCC (LE-FCC) which are designed with standard configurations of 14 TeV/3 ab⁻¹, 27 TeV/15 ab⁻¹, and 37.5 TeV/15 ab⁻¹. Madgraph in which the effective Lagrangian of the SM EFT is implemented using FeynRules and UFO framework is used to generate both background and signal events. These events are then passed through PYTHIA 8 for parton showering and Delphes to include realistic detector effects. After optimizing cuts on kinematics of three photons as well as the reconstructed invariant mass of the two leading photons, invariant mass of three leading photons is used to obtain constraints on the Wilson coefficients of dimension-six operators. We report on the result of a two-dimensional scan of \tilde{c}_γ and \tilde{c}_γ couplings at 95% confidence level and compare with the LHC results. Our obtained limits without systematic error on \tilde{c}_γ (\tilde{c}_γ) are $[-3.15; 1.41] \times 10^{-2}$ ($[-2.12; 2.12] \times 10^{-2}$), $[-1.21; 0.78] \times 10^{-2}$ ($[-0.98; 0.98] \times 10^{-2}$), and $[-0.89; 0.66] \times 10^{-2}$ ($[-0.77; 0.77] \times 10^{-2}$) for HL-LHC, HE-LHC, and LE-FCC, respectively.

DOI:10.5506/APhysPolB.52.1377

1. Introduction

Being the largest scientific instrument ever built, the Large Hadron Collider (LHC) with its discovery potential gave an opportunity to work in the physics of hadronic matter at extreme temperature and density for the large

* Funded by SCOAP³ under Creative Commons License, CC-BY 4.0.

[†] denizli_h@ibu.edu.tr

[‡] senol_a@ibu.edu.tr

particle physics community. With the discovery of Higgs boson [1, 2], Standard Model (SM) is completed and particle physics reaches an important moment in its history. Some of the crucial questions which are still not answered are: the nature of dark matter, the origin of the matter–antimatter asymmetry in the Universe, and the existence and hierarchy of neutrino masses. To address these questions and the properties of the newly discovered Higgs boson, the particle physics community decided to upgrade LHC by increasing its luminosity (rate of collisions) by a factor of five beyond the original design value and the integrated luminosity (total collisions created) by a factor of ten to sustain and extend its discovery potential. The possibility of building even higher energy frontier colliders is also under consideration. One can expect that these post-LHC circular high-energy hadron colliders will deepen our understanding of the origin of the electroweak symmetry breaking, Higgs couplings, and new physics.

The HL-LHC program aims at decreasing the statistical error in the measurements by half, while it will continue to examine the properties of Higgs boson and look for clues to explain the physics beyond SM [3]. The HL-LHC project includes a range of beam parameters and hardware configurations that will reach an integrated luminosity of approximately 250 fb^{-1} per year after upgrading, achieving a target of 3000 fb^{-1} at 7.0 TeV nominal beam energy reached by the LHC in a total of 12 years. One of the circular high-energy hadron colliders under consideration after HL-LHC is HE-LHC which will extend the current LHC center-of-mass energy by almost a factor of 2 and deliver an integrated luminosity of at least a factor of 3 larger than the HL-LHC [4]. It will use the existing LHC tunnel infrastructure and FCC-hh magnet technology, that is 16 Tesla dipole magnet. The other one is the LE-FCC [5], which is thought to minimize the cost of a future circular hadron collider housed in the FCC 100 km tunnel with 6 Tesla dipole magnet. This leads to a center-of-mass energy of 37.5 TeV. It plans to deliver an integrated luminosity of at least 10 ab^{-1} during a 20-year operation.

Measuring precisely the Higgs couplings has a great potential to give us detailed information on the new physics beyond the SM. The Effective Field Theory (EFT) approach is widely used in the search for possible deviations from the predictions of the Standard Model. In the EFT framework [6], new physics contributions beyond the SM are described by higher-dimensional operators in an expansion. These operators are invariant under the SM symmetries and suppressed by the new physics scale Λ . In this article, we investigate the potential for limitation of the EFT approach related to unitarity to describe possible contributions of the operators between Higgs and SM gauge boson at the High-Luminosity LHC (HL-LHC) as well as other post-LHC hadron–hadron colliders under consideration. These operators are extensively studied via different production mechanisms for hadron colliders [7–29].

One of the approaches would be to look for production which is rare in the SM. One production mechanism satisfying this in the hadron colliders involves events with three photons in the final state [30–32]. This process also implies pure electroweak interactions at the tree level. Therefore, the production mechanism stands out as an ideal platform to search for deviations from SM. In the literature, the three-photon final state as well as other mechanisms [33–36] are used in the search of anomalous Higgs couplings via EFT formalism. Either direct production or fragmentation process result in the three-photon final state in the hadron colliders. Since photons produced via direct production are typically isolated, requiring isolated photons will reduce the background contributions from the decays of unstable particles such as $\pi^0 \rightarrow \gamma\gamma$ and suppress the signal process with one or more fragmentation photons.

The organization of the paper is as follows. We highlight some details of the model that are relevant to our study and calculate the cross sections as a function of couplings under consideration for each post-LHC hadron colliders in Section 2. The discussion of kinematic cuts and the details of signal and background analysis are given in Section 3. In Section 4, we present obtained the sensitivity bounds on the \bar{c}_γ and \tilde{c}_γ couplings with a two-dimensional scan at 95% confidence level and compare them with the LHC results. Finally, we conclude in Section 5.

2. Theoretical framework of the effective operators

In this study, we are interested in the CP-conserving and CP-violating dimension-6 operators of the Higgs boson and electroweak gauge boson in the convention of the Strongly Interacting Light Higgs (SILH) basis in effective Lagrangian [37]. The CP-conserving dimension-6 operator between the Higgs boson and electroweak gauge bosons is defined in the general effective Lagrangian as follows:

$$\begin{aligned}
 \mathcal{L}_{\text{CPC}} = & \frac{\bar{c}_H}{2v^2} \partial^\mu [\Phi^\dagger \Phi] \partial_\mu [\Phi^\dagger \Phi] + \frac{\bar{c}_T}{2v^2} [\Phi^\dagger \overleftrightarrow{D}^\mu \Phi] [\Phi^\dagger \overleftrightarrow{D}_\mu \Phi] - \frac{\bar{c}_6 \lambda}{v^2} [\Phi^\dagger \Phi]^3 \\
 & - \left[\frac{\bar{c}_u}{v^2} y_u \Phi^\dagger \Phi \Phi^\dagger \bar{Q}_L u_R + \frac{\bar{c}_d}{v^2} y_d \Phi^\dagger \Phi \Phi \bar{Q}_L d_R + \frac{\bar{c}_l}{v^2} y_l \Phi^\dagger \Phi \Phi \bar{L}_L e_R + \text{h.c.} \right] \\
 & + \frac{ig}{m_W^2} \bar{c}_W [\Phi^\dagger T_{2k} \overleftrightarrow{D}^\mu \Phi] D^\nu W_{\mu\nu}^k + \frac{ig'}{2m_W^2} \bar{c}_B [\Phi^\dagger \overleftrightarrow{D}^\mu \Phi] \partial^\nu B_{\mu\nu} \\
 & + \frac{2ig}{m_W^2} \bar{c}_{HW} [D^\mu \Phi^\dagger T_{2k} D^\nu \Phi] W_{\mu\nu}^k + \frac{ig'}{m_W^2} \bar{c}_{HB} [D^\mu \Phi^\dagger D^\nu \Phi] B_{\mu\nu} \\
 & + \frac{g'^2}{m_W^2} \bar{c}_\gamma \Phi^\dagger \Phi B_{\mu\nu} B^{\mu\nu} + \frac{g_s^2}{m_W^2} \bar{c}_g \Phi^\dagger \Phi G_{\mu\nu}^a G_a^{\mu\nu}, \tag{1}
 \end{aligned}$$

where λ denotes the Higgs quartic coupling and Φ represents the Higgs sector containing a single $SU(2)_L$ doublet of fields; g_s , g , and g' are coupling constants of $SU(3)_C$, $SU(2)_L$, and $U(1)_Y$ gauge fields, respectively; the generators of $SU(2)_L$ in the fundamental representation are given by $T_{2k} = \sigma_k/2$ (here σ_k are the Pauli matrices); y_u , y_d , and y_l are the 3×3 Yukawa coupling matrices in flavor space; $\overleftrightarrow{D}_\mu$ correspond to the Hermitian derivative operators; $B^{\mu\nu}$, $W^{\mu\nu}$, and $G^{\mu\nu}$ are the electroweak and the strong field strength tensors, respectively.

The general effective Lagrangian can be extended with CP-violating operators in the SILH basis given below

$$\begin{aligned} \mathcal{L}_{\text{CPV}} = & \frac{ig}{m_W^2} \tilde{c}_{HW} D^\mu \Phi^\dagger T_{2k} D^\nu \Phi \tilde{W}_{\mu\nu}^k + \frac{ig'}{m_W^2} \tilde{c}_{HB} D^\mu \Phi^\dagger D^\nu \Phi \tilde{B}_{\mu\nu} \\ & + \frac{g'^2}{m_W^2} \tilde{c}_\gamma \Phi^\dagger \Phi B_{\mu\nu} \tilde{B}^{\mu\nu} + \frac{g_s^2}{m_W^2} \tilde{c}_g \Phi^\dagger \Phi G_{\mu\nu}^a \tilde{G}_a^{\mu\nu} \\ & + \frac{g^3}{m_W^2} \tilde{c}_{3W} \epsilon_{ijk} W_{\mu\nu}^i W_{\nu\rho}^j \tilde{W}^{\rho\mu k} + \frac{g_s^3}{m_W^2} \tilde{c}_{3G} f_{abc} G_{\mu\nu}^a G_{\nu\rho}^b \tilde{G}^{\rho\mu c}, \quad (2) \end{aligned}$$

where

$$\tilde{B}_{\mu\nu} = \frac{1}{2} \epsilon_{\mu\nu\rho\sigma} B^{\rho\sigma}, \quad \tilde{W}_{\mu\nu}^k = \frac{1}{2} \epsilon_{\mu\nu\rho\sigma} W^{\rho\sigma k}, \quad \tilde{G}_{\mu\nu}^a = \frac{1}{2} \epsilon_{\mu\nu\rho\sigma} G^{\rho\sigma a}$$

are the dual field strength tensors.

The dimension-6 CP-conserving (Eq. (1)) and CP-violating (Eq. (2)) operators in SILH bases can be defined in terms of the mass eigenstates after electroweak symmetry breaking. The relevant Higgs and neutral gauge boson couplings in the mass basis for triphoton production are given in the following Lagrangian:

$$\begin{aligned} \mathcal{L} = & -\frac{1}{4} g_{h\gamma\gamma} F_{\mu\nu} F^{\mu\nu} h - \frac{1}{4} \tilde{g}_{h\gamma\gamma} F_{\mu\nu} \tilde{F}^{\mu\nu} h \\ & - \frac{1}{4} g_{hzz}^{(1)} Z_{\mu\nu} Z^{\mu\nu} h - g_{hzz}^{(2)} Z_\nu \partial_\mu Z^{\mu\nu} h + \frac{1}{2} g_{hzz}^{(3)} Z_\mu Z^\mu h - \frac{1}{4} \tilde{g}_{hzz} Z_{\mu\nu} \tilde{Z}^{\mu\nu} h \\ & - \frac{1}{2} g_{haz}^{(1)} Z_{\mu\nu} F^{\mu\nu} h - \frac{1}{2} \tilde{g}_{haz} Z_{\mu\nu} \tilde{F}^{\mu\nu} h - g_{haz}^{(2)} Z_\nu \partial_\mu F^{\mu\nu} h, \quad (3) \end{aligned}$$

where the field strength tensors of Z -boson and photon are represented with $Z_{\mu\nu}$ and $F_{\mu\nu}$, respectively. The relationships between the effective couplings in the gauge basis and dimension-6 operators are given in Table I in which a_H coupling is the SM contribution to the $H\gamma\gamma$ vertex at loop level.

In order to simulate events involving the effect of the dimension-6 operators on the triphoton production mechanism in pp collisions with leading order, the effective Lagrangian of the SM EFT in Eq. (3) is implemented into

TABLE I

The relations between Lagrangian parameters in the mass basis (Eq. (3)) and the Lagrangian in gauge basis (Eqs. (1) and (2)) ($c_W \equiv \cos \theta_W$, $s_W \equiv \sin \theta_W$).

$$\begin{aligned}
 g_{h\gamma\gamma} &= a_H - \frac{8g\bar{c}_\gamma s_W^2}{m_W} \\
 \tilde{g}_{h\gamma\gamma} &= -\frac{8g\bar{c}_\gamma s_W^2}{m_W} \\
 g_{hzz}^{(1)} &= \frac{2g}{c_W^2 m_W} [\bar{c}_{HB} s_W^2 - 4\bar{c}_\gamma s_W^4 + c_W^2 \bar{c}_{HW}] \\
 g_{hzz}^{(2)} &= \frac{g}{c_W^2 m_W} [(\bar{c}_{HW} + \bar{c}_W) c_W^2 + (\bar{c}_B + \bar{c}_{HB}) s_W^2] \\
 g_{hzz}^{(3)} &= \frac{gm_W}{c_W^2} \left[1 - \frac{1}{2} \bar{c}_H - 2\bar{c}_T + 8\bar{c}_\gamma \frac{s_W^4}{c_W^2} \right] \\
 \tilde{g}_{hzz} &= \frac{2g}{c_W^2 m_W} [\bar{c}_{HB} s_W^2 - 4\bar{c}_\gamma s_W^4 + c_W^2 \tilde{c}_{HW}] \\
 g_{h\gamma z}^{(1)} &= \frac{gs_W}{c_W m_W} [\bar{c}_{HW} - \bar{c}_{HB} + 8\bar{c}_\gamma s_W^2] \\
 g_{h\gamma z}^{(2)} &= \frac{gs_W}{c_W m_W} [\bar{c}_{HW} - \bar{c}_{HB} - \bar{c}_B + \bar{c}_W] \\
 \tilde{g}_{h\gamma z} &= \frac{gs_W}{c_W m_W} [\tilde{c}_{HW} - \tilde{c}_{HB} + 8\tilde{c}_\gamma s_W^2]
 \end{aligned}$$

the MadGraph5_aMC@NLO v2.6.3.2 [38] event generator using FeynRules [39] and UFO [40] framework. The triphoton production process is sensitive to the Higgs-electroweak gauge boson couplings ($g_{h\gamma\gamma}$ and $g_{hz\gamma}$) and the couplings of a quark pair to single Higgs field (\tilde{y}_u and \tilde{y}_d) in the mass basis effective Lagrangian, the eight Wilson coefficients (\bar{c}_W , \bar{c}_B , \bar{c}_{HW} , \bar{c}_{HB} , \bar{c}_γ , \tilde{c}_{HW} , \tilde{c}_{HB} , and \tilde{c}_γ) related to Higgs-gauge boson couplings and also effective fermionic couplings in the gauge basis effective Lagrangian. Since the Yukawa coupling of the first- and second-generation fermions is very small, the effective fermionic couplings are ignored. The coupling constants other than \bar{c}_γ and \tilde{c}_γ couplings do not lead to considerable modifications in the cross section as seen in our previous work [36]. Thus in this study, we focus on the effect of \bar{c}_γ and \tilde{c}_γ couplings on the triphoton production process. We generate 64 samples to parametrize the cross-section function by varying two Wilson coefficients simultaneously for HL-LHC as well as other post-LHC hadron-hadron colliders under consideration. For the studies presented in this manuscript, we assume $\sqrt{s} = 14$ TeV with $L_{\text{int}} = 3 \text{ ab}^{-1}$ for HL-LHC, $\sqrt{s} = 27$ TeV with $L_{\text{int}} = 15 \text{ ab}^{-1}$ for HE-LHC, and $\sqrt{s} = 37.5$ TeV with $L_{\text{int}} = 15 \text{ ab}^{-1}$ for LE-FCC as indicated in Ref. [5]. We apply generator level cuts; $p_T^{\gamma_1, \gamma_2, \gamma_3} > 15$ GeV and $|\eta^{\gamma_1, 2, 3}| < 2.5$ in the calculations of the cross sections at the leading order. Then the method is validated by comparing the cross sections obtained with the parametrisation function to the cross section obtained from MadGraph5_aMC@NLO v2.6.3.2 with specific values of

the couplings. Figure 1 depicts the total cross section of $pp \rightarrow \gamma\gamma\gamma$ process as a function of the CP-conserving \bar{c}_γ couplings for $\tilde{c}_\gamma = 0$ and 0.05 in the right panel, and CP-violating \tilde{c}_γ couplings for $\bar{c}_\gamma = 0$ and 0.05 in the left panel at the three post-LHC circular colliders. In this figure, all effective couplings other than \bar{c}_γ and \tilde{c}_γ are set to zero. The effect of the \tilde{c}_γ is smaller in the cross section as a function of \bar{c}_γ in the right panel of Fig. 1, while \bar{c}_γ contribution in cross section is significant in the right panel of Fig. 1 in the range of the small coupling value of \tilde{c}_γ .

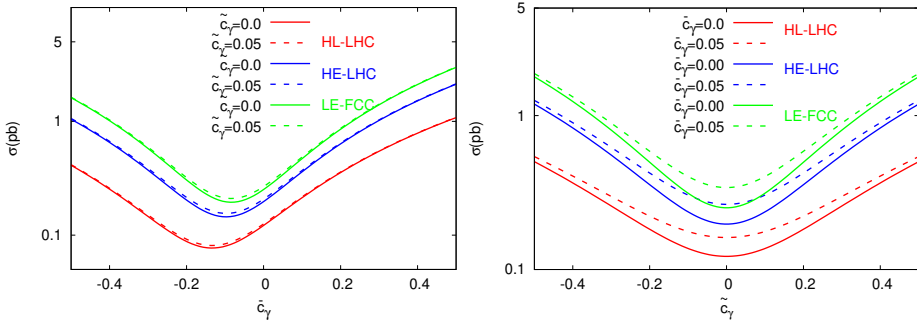


Fig. 1. The total cross section as a function of the CP-conserving \bar{c}_γ couplings for $\tilde{c}_\gamma = 0$ and 0.05 (left) and CP-violating \tilde{c}_γ couplings (right) for $\bar{c}_\gamma = 0$ and 0.05 $pp \rightarrow \gamma\gamma\gamma$ subprocess at the three post-LHC circular colliders.

3. Signal and background analysis

In this section, we give details of the simulation and the cut-based analysis steps to explore the potential of triphoton production to obtain limits on the anomalous Higgs boson \bar{c}_γ and \tilde{c}_γ couplings at $H\gamma\gamma$ and $HZ\gamma$ vertices in a model-independent Standard Model Effective Field Theory framework for the post-LHC circular high-energy hadron colliders. This final state consists of one energetic photon together with two photons originating from the Higgs boson decay. Therefore, the $pp \rightarrow \gamma\gamma\gamma$ process with non-zero \bar{c}_γ and \tilde{c}_γ effective couplings is considered as a signal including SM contribution as well as interference between effective couplings and SM contributions ($SB_{\gamma\gamma\gamma}$). The main sources of the SM background processes which are taken into account in this work are $pp \rightarrow \gamma\gamma\gamma$ ($B_{\gamma\gamma\gamma}$: the same final state as the signal process) and $pp \rightarrow \gamma\gamma + \text{jet}$ ($B_{\gamma\gamma j}$: in which jet may fake a photon). The MadGraph5_aMC@NLO v2.6.3.2 event generator is used to generate 500 k events for the signal and background processes at the leading order partonic level. The total of 64 samples for each post-LHC hadron collider consideration is generated by varying two Wilson coefficients \bar{c}_γ and \tilde{c}_γ simultaneously. Consequently, these events are passed through the PYTHIA 8 [41] including the initial and final parton shower and the fragmentation of partons into

hadron. The detector responses are taken into account with the card prepared for HL-LHC and HE-LHC studies released in Delphes 3.4.1 package [42]. Jets in all generated events are clustered by using FastJet [43] with anti- k_t algorithm where a cone radius is set as $\Delta R = 0.4$ [44]. All events are analysed by using the ExRootAnalysis utility [45] with ROOT [46].

Even though all three collider configurations expect to see pile-up effects in the range of several hundreds, we did not consider any pile-up effects since in this study we aim at giving an estimation to obtain the limits of effective Higgs couplings by post-LHC circular high-energy hadron collider options through the production of three photons [47]. We filtered events with at least three photons in the final state and jet veto to suppress jet-containing backgrounds for the analysis as a first step (Cut-1). Photons are ordered with respect to their transverse momentum. That is, γ_1 , γ_2 , and γ_3 are the first, second, and third leading photon, respectively ($p_T^{\gamma_1} > p_T^{\gamma_2} > p_T^{\gamma_3}$). Then, we review various kinematic variables of photons in order to use them in “cut-based” analysis and to achieve physical intuition. The phase space of the first, second, and third leading photons for the signal with values $\bar{c}_\gamma = 0.05$ and $\tilde{c}_\gamma = 0.05$ and the relevant SM backgrounds for HL-LHC, HE-LHC, and LE-FCC are shown in Fig. 2, Fig. 3, and Fig. 4, respectively. These phase

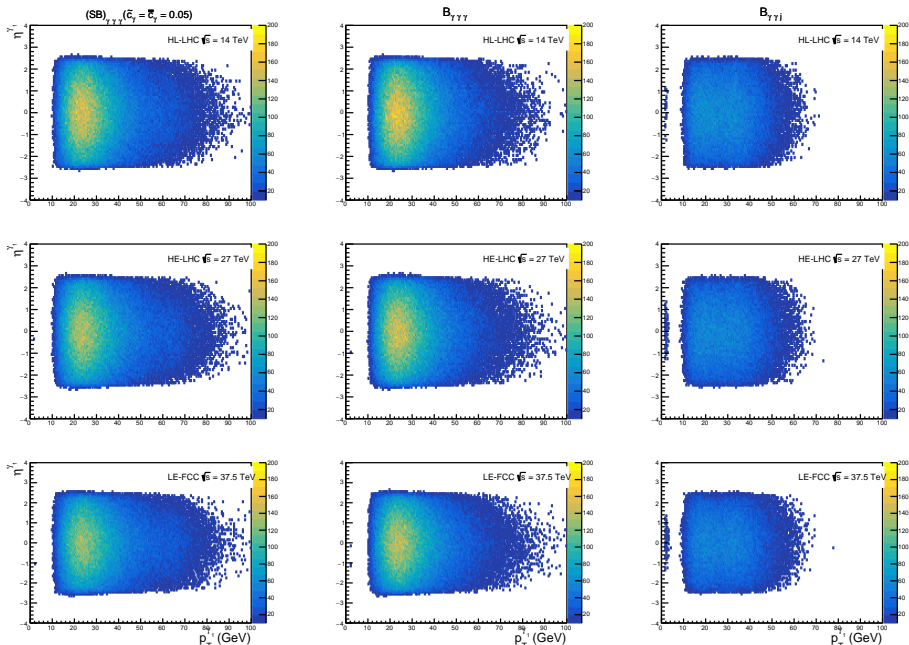


Fig. 2. The phase space of the leading photon for signal ($SB_{\gamma\gamma\gamma}$) including SM and their interference, SM background process (B_{SM}) with the same final state as signal and $B_{\gamma j j}$ in each column. Rows are for different post-LHC circular colliders.

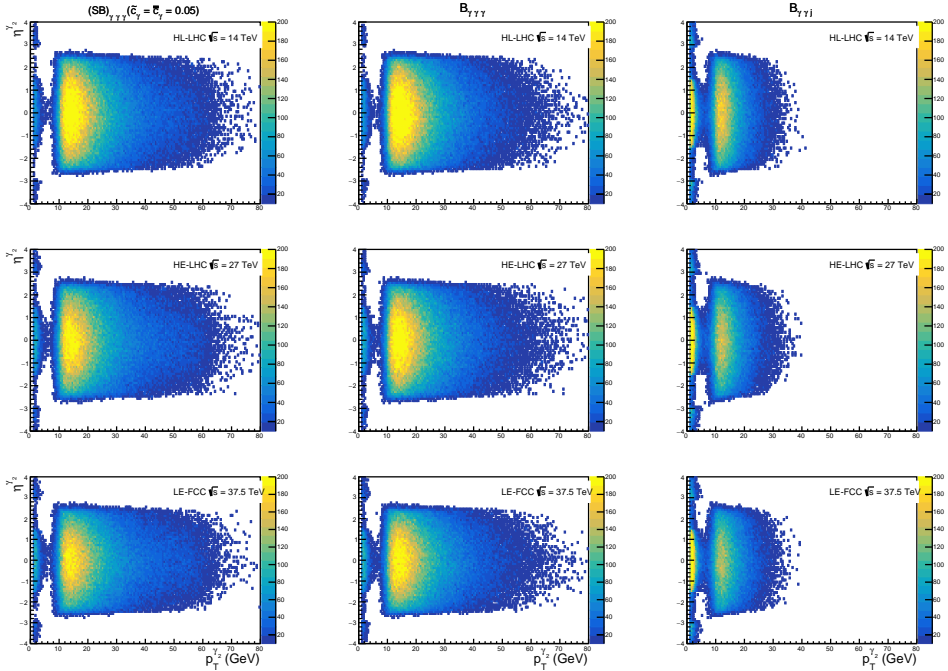


Fig. 3. The phase space of the second-leading photon for signal ($SB_{\gamma\gamma\gamma}$) including SM and their interference, SM background process (B_{SM}) with the same final state as signal and $B_{\gamma\gamma j}$ in each column. Rows are for different post-LHC circular colliders.

space distributions led us to the $p_T^{\gamma 1} > 50$ GeV, $p_T^{\gamma 2} > 35$ GeV, $p_T^{\gamma 3} > 12$ GeV, and $|\eta^{\gamma 1,2,3}| < 2.5$ region, where the signal process can be separated from the backgrounds (Cut-2 and Cut-3). The distance between each two photons is determined as $\Delta R(\gamma_i, \gamma_j) = [(\Delta\phi_{\gamma_i, \gamma_j})^2 + (\Delta\eta_{\gamma_i, \gamma_j})^2]^{1/2}$, where $\Delta\phi_{\gamma_i, \gamma_j}$ and $\Delta\eta_{\gamma_i, \gamma_j}$ are the azimuthal angle and the pseudo-rapidity difference between any two photons, respectively. A useful requirement to select isolated photons is to apply to the minimum distance between each two photons as $\Delta R(\gamma_1, \gamma_2) > 0.4$, $\Delta R(\gamma_1, \gamma_3) > 0.4$, $\Delta R(\gamma_2, \gamma_3) > 0.4$ (Cut-4). Having the targeted signature with three prompt photons, we consider an invariant mass of three-photon *versus* the invariant mass of two-photon are checked for the signal and the relevant SM backgrounds after Cut-4 at HL-LHC as well as other post-LHC hadron-hadron colliders under consideration. The distributions for signal with $\bar{c}_\gamma = \tilde{c}_\gamma = 0.05$ couplings and relevant SM backgrounds after Cut-4 (left-to-right) are given in Fig. 5, Fig. 6, and Fig. 7 for HL-LHC, HE-LHC, and LE-FCC, respectively.

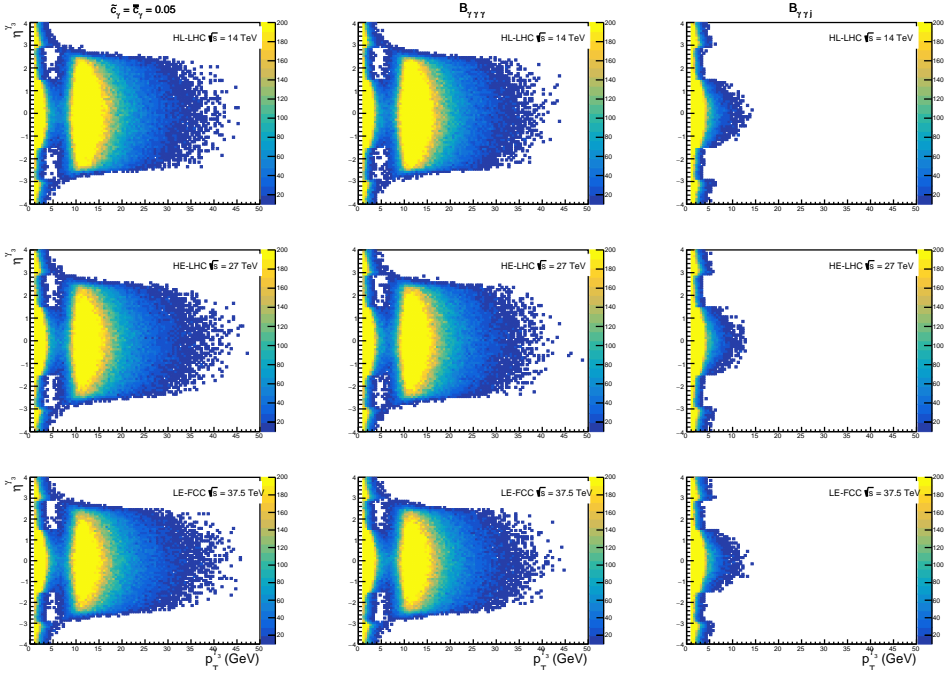


Fig. 4. The phase space of the third-leading photon for signal ($SB_{\gamma\gamma\gamma}$) including SM and their interference, SM background process ($B_{\gamma\gamma\gamma}$) with the same final state as signal and $B_{\gamma\gamma j}$ in each column. Rows are for different post-LHC circular colliders.

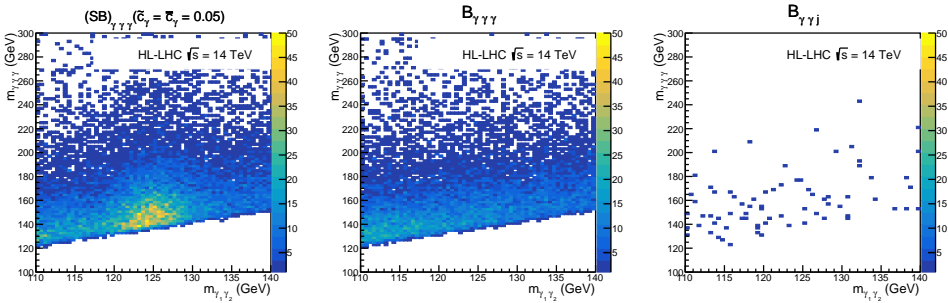


Fig. 5. The invariant mass of three-photon *versus* the invariant mass of two-photon distribution for signal ($\tilde{c}_\gamma = \tilde{c}_\gamma = 0.05$) and relevant SM backgrounds after Cut-4 for 14 TeV center-of-mass energy collider, namely HL-LHC (left-to-right).

We select events with the invariant mass of three-photon $m_{\gamma_1\gamma_2\gamma_3} > 160$ GeV (Cut-5). In order to focus on events where two photons are coming from the decay of Higgs boson, we consider a reconstructed invariant mass from two leading photons in the range of $122 \text{ GeV} < m_{\gamma\gamma} < 128$ GeV (Cut-6). A summary of the cuts used in the analysis is given in Table II. The distributions

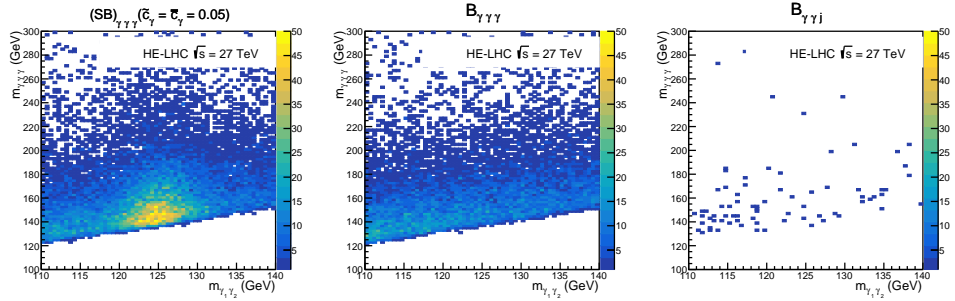


Fig. 6. The invariant mass of three-photon *versus* the invariant mass of two-photon distribution for signal ($\bar{c}_\gamma = \tilde{c}_\gamma = 0.05$) and relevant SM backgrounds after Cut-4 for 27 TeV center-of-mass energy collider, namely HE-LHC.

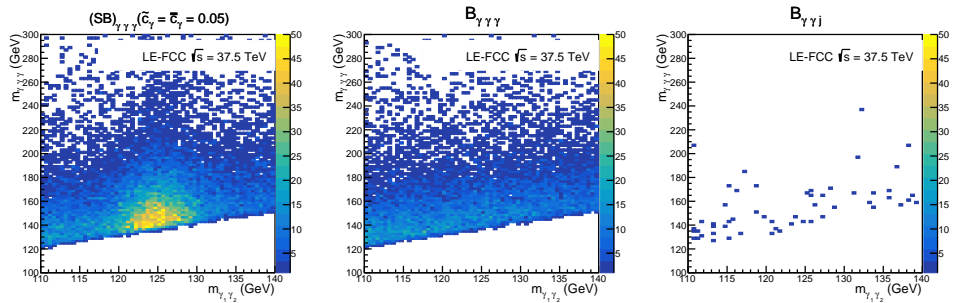


Fig. 7. The invariant mass of three-photon *versus* the invariant mass of two-photon distribution for signal ($\bar{c}_\gamma = \tilde{c}_\gamma = 0.05$) and relevant SM backgrounds after Cut-4 for 37.5 TeV center-of-mass energy collider, namely LE-FCC.

of the reconstructed invariant mass of two leading photons are presented for the signal plus total SM backgrounds $S + B_T$ ($\bar{c}_\gamma = \tilde{c}_\gamma = 0.05$) (light grey/red) and total SM background $B_T = B_{\gamma\gamma\gamma} + B_{\gamma\gamma j}$ (grey) as well as

TABLE II

List of optimized cuts considered in the analysis for selecting events to obtain limits.

Cuts	Definitions
Cut-1	$N_\gamma > 2, \quad N_{\text{jet}} = 0$
Cut-2	Cut-1 + $p_T^{\gamma_1} > 50 \text{ GeV}, \quad p_T^{\gamma_2} > 35 \text{ GeV}, \quad p_T^{\gamma_3} > 12 \text{ GeV}$
Cut-3	Cut-2 + $ \eta^{\gamma_{1,2,3}} < 2.5$
Cut-4	Cut-3 + $\Delta R(\gamma_1, \gamma_2) > 0.4, \quad \Delta R(\gamma_1, \gamma_3) > 0.4, \quad \Delta R(\gamma_2, \gamma_3) > 0.4$
Cut-5	Cut-4 + $m_{\gamma_1\gamma_2\gamma_3} > 160 \text{ GeV}$
Cut-6	Cut-5 + $122 \text{ GeV} < m_{\gamma\gamma} < 128 \text{ GeV}$

their ratio $(S + B_T)/B_T$ in Fig. 8 for HL-LHC, HE-LHC, and LE-FCC (left-to-right). Here, the main contribution comes from the $B_{\gamma\gamma\gamma}$ background. A number of events after this final cut are used to obtain limits on the anomalous Higgs effective couplings. A number of signal ($\bar{c}_\gamma = \tilde{c}_\gamma = 0.05$) and relevant background events normalized to the corresponding luminosities of 3 ab^{-1} , 15 ab^{-1} , and 15 ab^{-1} (HL-LHC, HE-LHC, and LE-FCC, respectively) after each cut are given in Table III. The efficiency of each cut step can be calculated from this table. The overall effect of the cuts used in Table III changes between 0.8% and 1.1% moving from HL-LHC to LE-FCC for $\bar{c}_\gamma = \tilde{c}_\gamma = 0.05$. On the other hand, the efficiency of cuts for SM backgrounds $B_{\gamma\gamma\gamma}$ and $B_{\gamma\gamma j}$ is 0.34% and 0.003%, respectively. The efficiency of the cuts also depends on the anomalous Higgs boson dimension-6 couplings value. We observed that efficiency gets lower to the 0.4% for the signal with couplings set to $\bar{c}_\gamma = \tilde{c}_\gamma = 0.01$. One might get better limits when cuts are optimized to each collider option.

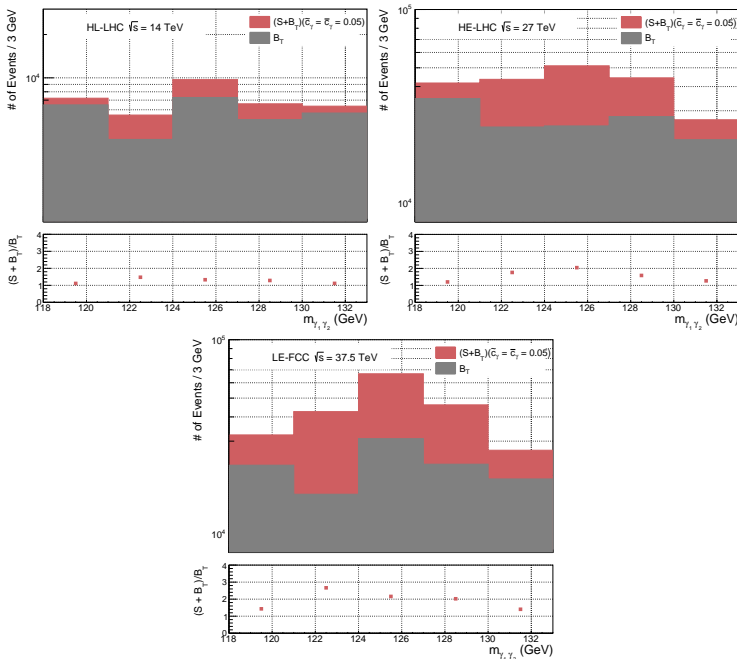


Fig. 8. (Colour on-line) The invariant mass distribution of two-photon after Cut-5 for $S + B_T$ ($\bar{c}_\gamma = \tilde{c}_\gamma = 0.05$) (light grey/red) and the total SM background B_T (grey) for HL-LHC, HE-LHC, and LE-FCC, respectively. These distributions are normalized to relevant L_{int} (3 ab^{-1} , 15 ab^{-1} , and 15 ab^{-1}).

TABLE III

A number of signal and relevant events after each cut used in the analysis with integrated luminosities of 3 ab^{-1} , 15 ab^{-1} , and 15 ab^{-1} for HL-LHC, HE-LHC, and LE-FCC, respectively.

Colliders	Process	Cut-1	Cut-2	Cut-3	Cut-4	Cut-5	Cut-6
HL-LHC	SB $_{\gamma\gamma\gamma}$ ($\bar{c}_\gamma = \tilde{c}_\gamma = 0.05$)	373073	54673.7	53502.3	53275.4	38071.9	2916.41
	$B_{\gamma\gamma\gamma}$	278456	36454.8	35640.1	35491.9	26282.3	954.18
	$B_{\gamma\gamma j}$	1.2704×10^8	158052	144823	139949	78677.8	3481.32
HE-LHC	SB $_{\gamma\gamma\gamma}$ ($\bar{c}_\gamma = \tilde{c}_\gamma = 0.05$)	2.91392×10^6	450225	440311	437960	310376	29650.2
	$B_{\gamma\gamma\gamma}$	2.13519×10^6	283158	276893	275816	205528	7306.28
	$B_{\gamma\gamma j}$	5.98137×10^8	710189	644044	637082	337688	20887.9
LE-FCC	SB $_{\gamma\gamma\gamma}$ ($\bar{c}_\gamma = \tilde{c}_\gamma = 0.05$)	3.61827×10^6	573519	559763	556825	395603	41175
	$B_{\gamma\gamma\gamma}$	2.63292×10^6	349711	341548	340030	254747	9522.67
	$B_{\gamma\gamma j}$	5.70719×10^8	696264	647526	633600	382945	13925.3

4. Sensitivity of the dimension-6 Higgs-gauge boson couplings

The χ^2 statistical analysis approach, which measures how the expectations are compared with the actual data observed (or model results), is used to obtain the sensitivity of the dimension-6 Higgs-gauge boson couplings in the $pp \rightarrow \gamma\gamma\gamma$ process as follows:

$$\chi^2 = \sum_i^{n_{\text{bins}}} \left(\frac{N_i^{\text{NP}} - N_i^{\text{B}}}{N_i^{\text{B}} \Delta_i} \right)^2, \quad (4)$$

where N_i^{NP} is the total number of events in the existence of effective couplings (S), the number of events of relevant SM backgrounds in i^{th} bin of the invariant mass distributions of reconstructed Higgs boson from two leading photons denotes N_i^{B} , $\Delta_i = \sqrt{\delta_{\text{sys}}^2 + \frac{1}{N_i^{\text{B}}}}$ is the combined systematic (δ_{sys}) and statistical errors in each bin. In this analysis, we focused on \bar{c}_γ and \tilde{c}_γ couplings which are the main coefficients contributing to the $pp \rightarrow \gamma\gamma\gamma$ signal process. In the two-dimensional χ^2 analysis, two Higgs-gauge boson couplings \bar{c}_γ and \tilde{c}_γ are assumed to deviate from their SM values simultaneously, while all other Wilson coefficients are set to zero. In Fig. 9, we show 95% C.L. contours for anomalous \bar{c}_γ and \tilde{c}_γ couplings with integrated luminosities of 3 ab^{-1} , 15 ab^{-1} , and 15 ab^{-1} for HL-LHC, HE-LHC, and LE-FCC without systematic errors. As we can see from Fig. 9, the best limits with-

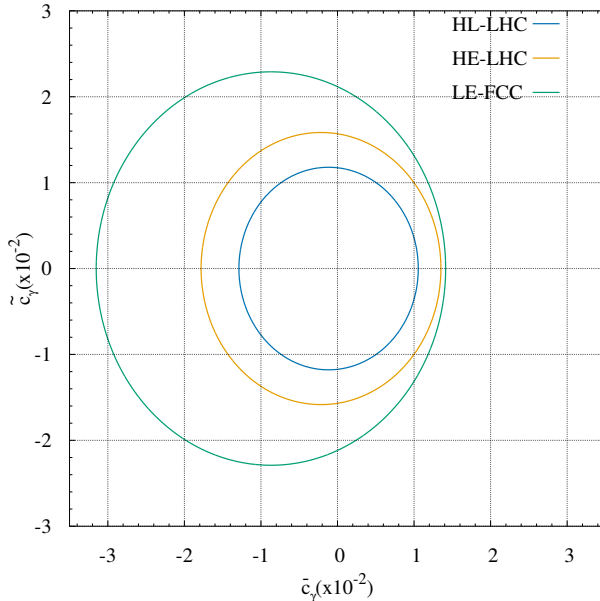


Fig. 9. Two-dimensional 95% C.L. intervals on the plane for \bar{c}_γ and \tilde{c}_γ without the systematic errors for HL-LHC, HE-LHC, and LE-FCC taking $L_{\text{int}} = 3, 15,$ and 15 ab^{-1} respectively. The limits are derived with all other coefficients set to zero.

out the systematic error on dimension-6 Higgs-gauge boson couplings \bar{c}_γ (\tilde{c}_γ) couplings are $[-3.15; 1.41] \times 10^{-2}$ ($[-2.12; 2.12] \times 10^{-2}$), $[-1.21; 0.78] \times 10^{-2}$ ($[-0.98; 0.98] \times 10^{-2}$), and $[-0.89; 0.66] \times 10^{-2}$ ($[-0.77; 0.77] \times 10^{-2}$) for HL-LHC, HE-LHC, and LE-FCC, respectively. In Fig. 10, we also present the same contour plot taking into account the systematic error for HL-LHC, HE-LHC, and LE-FCC, respectively. The limits on \bar{c}_γ and \tilde{c}_γ couplings get worse when systematic errors are increased in each hadron collider considered in this study. For example, when $\delta_{\text{sys}} = 3\%$, the limits on \bar{c}_γ (\tilde{c}_γ) couplings are $[-1.67; 1.67] \times 10^{-2}$ ($[-1.69; 1.69] \times 10^{-2}$) for LE-FCC collider with 15 ab^{-1} of integrated luminosity. These limits are up to 2 times worse than those obtained without systematic errors as seen from Fig. 10. The ATLAS experiment probed limits on these couplings by using a fit to five measured differential cross sections in $H \rightarrow \gamma\gamma$ decay channel [22]. They obtained $[-7.4; 5.7] \times 10^{-4} \cup [3.8; 5.1] \times 10^{-3}$ and $[-1.8; 1.8] \times 10^{-3}$ limits on \bar{c}_γ and \tilde{c}_γ , respectively with an integrated luminosity of 20.3 fb^{-1} at $\sqrt{s} = 8 \text{ TeV}$, respectively. In their similar analysis on 13 TeV center-of-mass energy with an integrated luminosity of 36.1 fb^{-1} , they claim that $H \rightarrow \gamma\gamma$ decay channel is not sensitive to \bar{c}_γ and \tilde{c}_γ [29]. Results of the analysis with increased luminosity ($L_{\text{int}} = 139 \text{ fb}^{-1}$) at $\sqrt{s} = 13 \text{ TeV}$ by the ATLAS Collaboration are $[-1.1; 1.1] \times 10^{-4}$ and $[-2.8; 4.3] \times 10^{-4}$ for \bar{c}_γ and \tilde{c}_γ , respectively [48].

In our study, limitations are placed on dimension-6 operators by focusing only on three-photon production in the post-LHC scenarios. One can obtain stringent bounds on these operators by taking into account other decay channels of the Higgs boson as in Refs. [22, 29, 48]. Furthermore, it is also possible to include the three-photon analysis in global fit with other production processes to achieve limits on dimension-6 operators with greater precision.

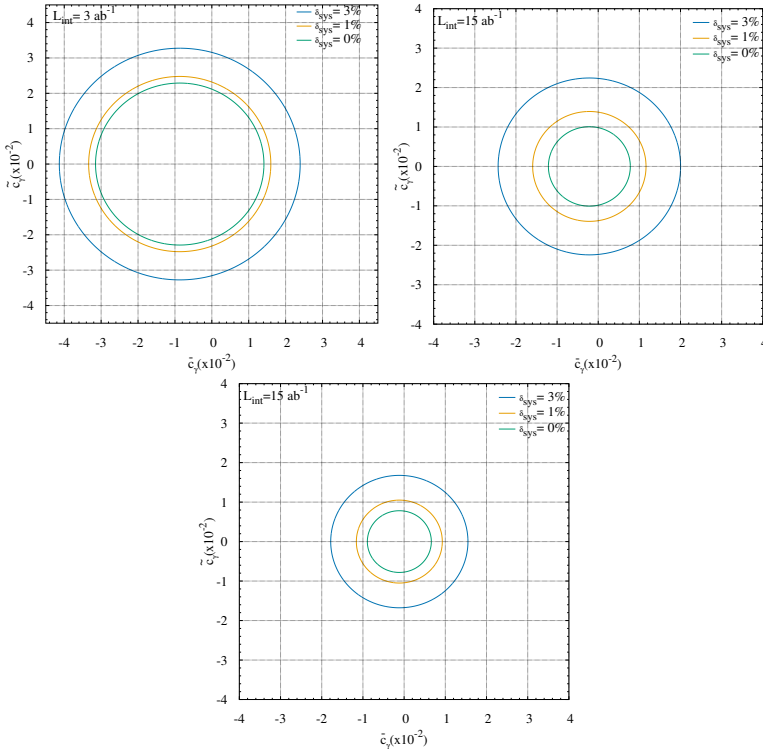


Fig. 10. Two-dimensional 95% C.L. intervals on the \bar{c}_γ and \tilde{c}_γ couplings plane considering 0, 1%, and 3% systematic error at HL-LHC, HE-LHC, and LE-FCC (left-to-right). The limits are derived with all coefficients other than \bar{c}_γ and \tilde{c}_γ set to zero.

5. Conclusions

The potential of $pp \rightarrow \gamma\gamma\gamma$ process is investigated to obtain limits on the \bar{c}_γ and \tilde{c}_γ couplings at 95% confidence level at High-Luminosity LHC (HL-LHC) as well as other post-LHC hadron-hadron colliders under consideration (14 TeV/3 ab^{-1} , 27 TeV/15 ab^{-1} , and 37.5 TeV/15 ab^{-1} , respectively). The signal (non-zero couplings) including interference with SM

and both background events are generated in MadGraph where the effective Lagrangian of the SM EFT is implemented using FeynRules and UFO framework. Then, events are passed through PYTHIA 8 for parton showering and hadronization, and Delphes to include realistic detector effects. 64 samples for each hadron collider consideration are generated by varying two Wilson coefficients simultaneously to obtain sensitivity bounds on the couplings. The targeted signature consists of three prompt photons. Therefore, 2D plots of kinematic variables pseudo-rapidity *versus* transverse momentum of each photon and invariant mass distributions of three-photon as a function of the reconstructed invariant mass of two leading photons are plotted to determine a cut-based analysis. To identify the signal over background, we made a series of standard cuts on the transverse momentum and pseudorapidity of three leading photon as well as photon separation ΔR . We also apply a cut on invariant mass of a two-photon system reconstructed from two leading photons. Finally, we use transverse momentum of the three-photon system for χ^2 analysis to obtain limits. The reconstructed invariant mass of three-photon in the range of Higgs-boson reconstructed from two leading photons is used to obtain limits on the anomalous Higgs effective couplings in the $pp \rightarrow \gamma\gamma\gamma$ signal process and the relevant SM background. Our obtained limits without systematic error on \tilde{c}_γ (\tilde{c}_γ) are $[-3.15; 1.41] \times 10^{-2}$ ($[-2.12; 2.12] \times 10^{-2}$), $[-1.21; 0.78] \times 10^{-2}$ ($[-0.98; 0.98] \times 10^{-2}$), and $[-0.89; 0.66] \times 10^{-2}$ ($[-0.77; 0.77] \times 10^{-2}$) for HL-LHC, HE-LHC, LE-FCC, respectively. No discussion of possible sources of systematic uncertainty is given in the manuscript. However, its effects on the limits of the couplings are considered. Results including systematic errors get worse as expected. Nevertheless, we predict the testable bounds from these post-LHC colliders via triphoton production on the anomalous Higgs boson couplings even with 1% systematic uncertainty from possible experimental sources.

This work was partially supported by the Turkish Atomic Energy Authority (TAEK) under grant No. 2018TAEK(CERN)A5.H6.F2-20.

REFERENCES

- [1] ATLAS Collaboration (G. Aad *et al.*), «Observation of a new particle in the search for the Standard Model Higgs boson with the ATLAS detector at the LHC», *Phys. Lett. B* **716**, 1 (2012), [arXiv:1207.7214 \[hep-ex\]](#).
- [2] CMS Collaboration (S. Chatrchyan *et al.*), «Observation of a new boson at a mass of 125 GeV with the CMS experiment at the LHC», *Phys. Lett. B* **716**, 30 (2012), [arXiv:1207.7235 \[hep-ex\]](#).

- [3] G. Apollinari *et al.*, «High-Luminosity Large Hadron Collider (HL-LHC): Technical Design Report V. 0.1», *CERN Yellow Rep. Monogr.* **4**, 1 (2017).
- [4] FCC Collaboration (A. Abada *et al.*), «HE-LHC: The High-Energy Large Hadron Collider: Future Circular Collider Conceptual Design Report Volume 4», *Eur. Phys. J. ST* **228**, 1109 (2019).
- [5] M. Mangano, «Physics potential of a low-energy FCC-hh», CERN-FCC-PHYS-2019-0001, <https://cds.cern.ch/record/2681366>
- [6] W. Büchmüller, D. Wyler, «Effective lagrangian analysis of new interactions and flavour conservation», *Nucl. Phys. B* **268**, 621 (1986).
- [7] K. Hagiwara, R. Szalapski, D. Zeppenfeld, «Anomalous Higgs boson production and decay», *Phys. Lett. B* **318**, 155 (1993), [arXiv:hep-ph/9308347](https://arxiv.org/abs/hep-ph/9308347).
- [8] T. Corbett, O.J.P. Éboli, J. Gonzalez-Fraile, M.C. Gonzalez-Garcia, «Robust determination of the Higgs couplings: Power to the data», *Phys. Rev. D* **87**, 015022 (2013), [arXiv:1211.4580](https://arxiv.org/abs/1211.4580) [hep-ph].
- [9] J. Ellis, V. Sanz, T. You, «The Effective Standard Model after LHC Run I», *J. High Energy Phys.* **1503**, 157 (2015), [arXiv:1410.7703](https://arxiv.org/abs/1410.7703) [hep-ph].
- [10] J. Ellis, V. Sanz, T. You, «Complete Higgs sector constraints on dimension-6 operators», *J. High Energy Phys.* **1407**, 036 (2014), [arXiv:1404.3667](https://arxiv.org/abs/1404.3667) [hep-ph].
- [11] A. Falkowski, «Effective field theory approach to LHC Higgs data», *Pramana* **87**, 39 (2016), [arXiv:1505.00046](https://arxiv.org/abs/1505.00046) [hep-ph].
- [12] T. Corbett *et al.*, «The Higgs legacy of the LHC Run I», *J. High Energy Phys.* **1508**, 156 (2015), [arXiv:1505.05516](https://arxiv.org/abs/1505.05516) [hep-ph].
- [13] F. Ferreira, B. Fuks, V. Sanz, D. Sengupta, «Probing CP-violating Higgs and gauge-boson couplings in the Standard Model effective field theory», *Eur. Phys. J. C* **77**, 675 (2017), [arXiv:1612.01808](https://arxiv.org/abs/1612.01808) [hep-ph].
- [14] V. Khachatryan *et al.*, «Constraints on the spin-parity and anomalous HVV couplings of the Higgs boson in proton collisions at 7 and 8 TeV», *Phys. Rev. D* **92**, 012004 (2015), [arXiv:1411.3441](https://arxiv.org/abs/1411.3441) [hep-ex].
- [15] V. Khachatryan *et al.*, «Combined search for anomalous pseudoscalar HVV couplings in $VH(H \rightarrow b\bar{b})$ production and $H \rightarrow VV$ decay», *Phys. Lett. B* **759**, 672 (2016), [arXiv:1602.04305](https://arxiv.org/abs/1602.04305) [hep-ex].
- [16] H. Khanpour, S. Khatibi, M. Mohammadi Najafabadi, «Probing Higgs boson couplings in $H + \gamma$ production at the LHC», *Phys. Lett. B* **773**, 462 (2017), [arXiv:1702.05753](https://arxiv.org/abs/1702.05753) [hep-ph].
- [17] S. von Buddenbrock *et al.*, «Multi-lepton signatures of additional scalar bosons beyond the Standard Model at the LHC», *J. Phys. G: Nucl. Part. Phys.* **45**, 115003 (2018), [arXiv:1711.07874](https://arxiv.org/abs/1711.07874) [hep-ph].
- [18] L. Shi, Z. Liang, B. Liu, Z. He, «Constraining the anomalous Higgs boson coupling in $H + \gamma$ production», *Chinese Phys. C* **43**, 043001 (2019), [arXiv:1811.02261](https://arxiv.org/abs/1811.02261) [hep-ph].

- [19] F.F. Freitas, C.K. Khosa, V. Sanz, «Exploring the standard model EFT in VH production with machine learning», *Phys. Rev. D* **100**, 035040 (2019), [arXiv:1902.05803 \[hep-ph\]](#).
- [20] ATLAS Collaboration (M. Aaboud *et al.*), «Measurement of $VH, H \rightarrow b\bar{b}$ production as a function of the vector-boson transverse momentum in 13 TeV pp collisions with the ATLAS detector», *J. High Energy Phys.* **1905**, 141 (2019), [arXiv:1903.04618 \[hep-ex\]](#).
- [21] S. Banerjee, F. Krauss, M. Spannowsky, «Revisiting the $t\bar{t}hh$ channel at the FCC-hh», *Phys. Rev. D* **100**, 073012 (2019), [arXiv:1904.07886 \[hep-ph\]](#).
- [22] ATLAS Collaboration (G. Aad *et al.*), «Constraints on non-Standard Model Higgs boson interactions in an effective Lagrangian using differential cross sections measured in the $H \rightarrow \gamma\gamma$ decay channel at $\sqrt{s} = 8$ TeV with the ATLAS detector», *Phys. Lett. B* **753**, 69 (2016), [arXiv:1508.02507 \[hep-ex\]](#).
- [23] C. Englert, R. Kogler, H. Schulz, M. Spannowsky, «Higgs coupling measurements at the LHC», *Eur. Phys. J. C* **76**, 393 (2016), [arXiv:1511.05170 \[hep-ph\]](#).
- [24] A. Buckley *et al.*, «Constraining top quark effective theory in the LHC Run II era», *J. High Energy Phys.* **1604**, 015 (2016), [arXiv:1512.03360 \[hep-ph\]](#).
- [25] C. Englert, R. Rosenfeld, M. Spannowsky, A. Tonero, «New physics and signal-background interference in associated $pp \rightarrow HZ$ production», *Eur. Phys. Lett.* **114**, 31001 (2016), [arXiv:1603.05304 \[hep-ph\]](#).
- [26] C. Degrande *et al.*, «Electroweak Higgs boson production in the standard model effective field theory beyond leading order in QCD», *Eur. Phys. J. C* **77**, 262 (2017), [arXiv:1609.04833 \[hep-ph\]](#).
- [27] F. Bishara, R. Contino, J. Rojo, «Higgs pair production in vector-boson fusion at the LHC and beyond», *Eur. Phys. J. C* **77**, 481 (2017), [arXiv:1611.03860 \[hep-ph\]](#).
- [28] L.S. Ling *et al.*, «Dimension-six operators in Higgs boson pair production via vector-boson fusion at the LHC», *Phys. Rev. D* **96**, 055006 (2017), [arXiv:1708.04785 \[hep-ph\]](#).
- [29] ATLAS Collaboration (M. Aaboud *et al.*), «Measurements of Higgs boson properties in the diphoton decay channel with 36 fb^{-1} of pp collision data at $\sqrt{s} = 13$ TeV with the ATLAS detector», *Phys. Rev. D* **98**, 052005 (2018), [arXiv:1802.04146 \[hep-ex\]](#).
- [30] F. de Campos *et al.*, «Testing anomalous Higgs couplings in triple photon production at the Tevatron collider», *Phys. Lett. B* **435**, 407 (1998), [arXiv:hep-ph/9806307](#).
- [31] M.C. Gonzalez-Garcia, «Anomalous Higgs couplings», *Int. J. Mod. Phys. A* **14**, 3121 (1999), [arXiv:hep-ph/9902321](#).
- [32] ATLAS Collaboration (M. Aaboud *et al.*), «Measurement of the production cross section of three isolated photons in pp collisions at $\sqrt{s} = 8$ TeV using the ATLAS detector», *Phys. Lett. B* **781**, 55 (2018), [arXiv:1712.07291 \[hep-ex\]](#).

- [33] L3 Collaboration (P. Achard *et al.*), «Search for anomalous couplings in the Higgs sector at LEP», *Phys. Lett. B* **589**, 89 (2004), [arXiv:hep-ex/0403037](#).
- [34] DELPHI Collaboration (P. Abreu *et al.*), «Search for the Higgs boson in events with isolated photons at LEP 2», *Phys. Lett. B* **458**, 431 (1999).
- [35] ALEPH Collaboration (A. Heister *et al.*), «Search for gamma gamma decays of a Higgs boson in e^+e^- collisions at s up to 209 GeV», *Phys. Lett. B* **544**, 16 (2002).
- [36] H. Denizli, K. Oyulmaz, A. Senol, «Testing for observability of Higgs effective couplings in triphoton production at FCC-hh», *J. Phys. G: Nucl. Part. Phys.* **46**, 105007 (2019), [arXiv:1901.04784 \[hep-ph\]](#).
- [37] A. Alloul, B. Fuks, V. Sanz, «Phenomenology of the Higgs Effective Lagrangian via FeynRules», *J. High Energy Phys.* **1404**, 110 (2014), [arXiv:1310.5150 \[hep-ph\]](#).
- [38] J. Alwall *et al.*, «The automated computation of tree-level and next-to-leading order differential cross sections, and their matching to parton shower simulations», *J. High Energy Phys.* **1407**, 079 (2014), [arXiv:1405.0301 \[hep-ph\]](#).
- [39] A. Alloul *et al.*, «FeynRules 2.0 — A complete toolbox for tree-level phenomenology», *Comput. Phys. Commun.* **185**, 2250 (2014), [arXiv:1310.1921 \[hep-ph\]](#).
- [40] C. Degrande *et al.*, «UFO — The Universal FeynRules Output», *Comput. Phys. Commun.* **183**, 1201 (2012), [arXiv:1108.2040 \[hep-ph\]](#).
- [41] T. Sjöstrand *et al.*, «An Introduction to PYTHIA 8.2», *Comput. Phys. Commun.* **191**, 159 (2015), [arXiv:1410.3012 \[hep-ph\]](#).
- [42] DELPHES 3 Collaboration (J. de Favereau *et al.*), «DELPHES 3: a modular framework for fast simulation of a generic collider experiment», *J. High Energy Phys.* **1402**, 057 (2014), [arXiv:1307.6346 \[hep-ex\]](#).
- [43] M. Cacciari, G.P. Salam, G. Soyez, «FastJet User Manual», *Eur. Phys. J. C* **72**, 1896 (2012), [arXiv:1111.6097 \[hep-ph\]](#).
- [44] M. Cacciari, G.P. Salam, G. Soyez, «The anti- k_t jet clustering algorithm», *J. High Energy Phys.* **0804**, 063 (2008), [arXiv:0802.1189 \[hep-ph\]](#).
- [45] <http://madgraph.hep.uiuc.edu/Downloads/ExRootAnalysis>
- [46] R. Brun, F. Rademakers, «ROOT — An object oriented data analysis framework», *Nucl. Instrum. Methods Phys. Res. A* **389**, 81 (1997).
- [47] M.L. Mangano, G. Ortona, M. Selvaggi, «Measuring the Higgs self-coupling via Higgs-pair production at a 100 TeV p - p collider», *Eur. Phys. J. C* **80**, 1030 (2020), [arXiv:2004.03505 \[hep-ph\]](#).
- [48] ATLAS Collaboration, «Measurements and interpretations of Higgs-boson fiducial cross sections in the diphoton decay channel using 139 fb $^{-1}$ of pp collision data at $\sqrt{s} = 13$ TeV with the ATLAS detector», ATLAS-CONF-2019-029.